EARTH SYSTEM DYNAMICS: THE DETERMINATION AND INTERPRETATION OF THE GLOBAL ANGULAR MOMENTUM BUDGET USING THE EARTH OBSERVING SYSTEM

Homepage: http://www.csr.utexas.edu/eos.html/

ABSTRACT

The objective of this investigation has been to examine the mass and momentum exchange between the atmosphere, oceans, solid Earth, hydrosphere, and cryosphere. The investigation has focused on changes in the Earth's gravity field, its rotation rate, atmospheric and oceanic circulation, global sea level change, ice sheet change, and global ground water circulation observed by contemporary sensors and models. The primary component of the mass exchange is water. The geodetic observables provided by these satellite sensors are used to study the transport of water mass in the hydrological cycle from one component of the Earth to another, and they are also used to evaluate the accuracy of models. As such, the investigation is concerned with the overall global water cycle. This report provides a description of scientific, educational and programmatic activities conducted during the period July 1, 1999 through June 30, 2000.

Research has continued into measurements of time-varying gravity and its relationship to Earth rotation. Variability of angular momentum and the related excitation of polar motion and Earth rotation have been examined for the atmosphere and oceans at time-scales of weeks to several years. To assess the performance of hydrologic models, we have compared geodetic signals derived from them with those observed by satellites. One key component is the interannual mass variability of the oceans obtained by direct observations from altimetry after removing steric signals. Further studies have been conducted on the steric model to quantify its accuracy at global and basin-scales. The results suggest a significant loss of water mass from the oceans to the land on time-scales longer than 1-year. These signals are not reproduced in any of the models, which have poorly determined interannual fresh water fluxes. Output from a coupled atmosphere-ocean model testing long-term climate change hypotheses has been compared to simulated errors from the Gravity Recovery and Climate Experiment (GRACE) mission. Results indicate that GRACE will be able to observe seasonal signals at half-wavelengths ranging from 1000 to 10000 km, and may be able to observe secular trends at half-wavelengths of greater than 2000-3000 km for soil moisture and snow depth if they are as large as some of the climate experiments predict.

1. INVESTIGATION OBJECTIVES

Momentum and mass transport between the atmosphere, oceans, cryosphere and solid Earth produce changes in the Earth's rotation, gravity field, atmospheric and ocean circulation, and global mean sea level. These changes are being measured with

unprecedented accuracy by current space geodetic techniques. Changes in Earth rotation are attributable to atmospheric winds and pressure, currents and pressure in the oceans, and mass redistribution within the Earth system components. Changes in the gravity field, which can be inferred from satellite orbit perturbations, arise only from mass redistribution. Sea level changes occur from both mass redistribution and ocean temperature change. The general ocean circulation is driven by the atmospheric forcing resulting in both mass and heat redistribution.

The mechanisms for the mass and momentum exchange between the components of the Earth's dynamic system are not fully understood. A primary focus of this research has been to clarify the mechanisms that dynamically couple the atmosphere, oceans, and solid Earth. Space-geodetic measurements provide global measures of momentum and mass redistribution and are of singular importance in studying the mechanisms involved in these changes. It is the objective of this investigation to use satellite-derived measurements of these quantities to: (1) observe, separate, and interpret these global signals, (2) provide results for evaluating the accuracies of current atmospheric and ocean general circulation models, and (3) , improve the predictive capabilities of global change models by increasing our understanding of the mechanisms involved in the mass and energy exchange.

Current satellite missions are able to measure mass and momentum changes at only the longest wavelengths. This investigation has focused for several years on global or integrated parameters to quantify mass and momentum change. Recently, we have begun to investigate the variations at shorter wavelengths and to compare satellite measurements with output from numerical models.

The progress during the past year is summarized in the following sections. The major topics covered are: (1) long-wavelength gravity variations, (2) Earth rotation variability and its relationship to gravity variations, (3) atmospheric and oceanic angular momentum variability and accuracy, and its relationship to Earth rotation/polar motion, (4) seasonal mass variability in hydrology models, (5) ocean steric model and ocean mass variations, and (6) mass signals observable by GRACE. Finally, the educational contributions of our investigation are described.

2. SCIENTIFIC ACTIVITIES
2.1 Long-Wavelength Gravity Field Variations

Beginning with the overall observations of the time-varying gravity, we have continued our studies of the long-wavelength components that can be detected with current geodetic satellites. A new solution for the secular changes in the zonal terms j_n (n = 2, 3, 4, 5, 6, 7 and 8) has been determined from Starlette, Lageos-1, Lageos-2, Ajisai, Etalon 1 and 2, Stella, and BE-C using the entire data set for each satellite covering the time period through the end of 1997 with the longest time span of over 23 years [Cheng and Tapley, 1999a, Cheng et al., 1999]. Corrections to a reference gravity model (TEG-3) to degree and order 5 were estimated for each 30-days, using the SLR data from 6 satellites and DORIS data from 2 satellites: TOPEX and SPOT2. We have

begun to study the secular and seasonal variations in the low degree coefficients, with particular emphasis on the non-zonal terms. Figure 1 shows the monthly solution of the J2 variation from the multi-satellite solutions during a span of 25 years (3/1975-3/2/2000). The observed seasonal variation in J2 is in good agreement with predictions from current models of the mass redistribution in the atmosphere, ground water and ocean [Cheng and Tapley, 1999b]. In addition, the geoid determined from the solutions has annual amplitudes similar to those resulting from the geophysical models and previous SLR solutions [Nerem et al., 2000].

The previous study of the time-varying geoid [Nerem et al., 2000] was limited to seasonal signals, as a seasonally varying coefficients were estimated along with a mean gravity field. The new solution, however, can be used to study variability at other periods, because of the 30-day solutions. During the subsequent investigation interval we will study the sub-annual and interannual variations to quantify the size of changes observable by the GRACE mission, which is scheduled to be launched in 2001. If the 30-day solutions prove to be of sufficient accuracy compared to the GRACE measurements, we can begin to study decadal variations in water mass storage at the longest wavelengths.

2.2 Earth Rotation and Angular Momentum

The Earth rotational variations can be summarized in three parameters: the equatorial components, or changes in the motion of the pole's location (X, Y), and the axial component, related to changes in the length of day (LOD). For all three components the excitations from changes in angular momentum may be divided into the effects of mass and motion. The mass variations are be related to changes of atmospheric surface pressure, continental water storage, and non-steric sea level change. The motion terms relate to the variations of winds and currents In addition, the mechanisms relating the transfer of angular mometum between the geophysical fluids and the solid Earth, namely the torques are of interest as well.   We have examined several topics related to Earth rotation in the last year. The major results are summarized in the following sections.

2.2.1 Relationship between Earth Rotation and Gravitational Change

The mass-associated excitations of X, Y, and LOD are proportional to the degree 2 spherical harmonics C21, S21, and C20, respectively [Lambeck, 1980] and, therefore, provide a means to infer the degree 2 gravitational variations in C21, S21, and C20 from observed Earth rotational changes. One can then compare the estimates with those measured by satellite laser ranging to geodetic satellites such as LAGEOS, which is the most accurate means in detecting planetary scale gravitational variations at the present. One benefit of this study is that it will provide observational constraints to the gravity determined from the future GRACE mission, in addition to the LAGEOS SLR measurements. Another benefit is that it will provide a chance to detect high frequency (e.g. sub-monthly) variations in the degree 2 gravity fields, which are not detectable from either LAGEOS SLR data or the GRACE observation, which will compute a gravity field approximately every 30 days. For details of formulations, geophysical models, Earth rotational observations, and computations, see Chen et al. [2000a].

3

The C21, S21, and C20 variations estimated from SPACE 97 [Gross, 1996] Earth rotational observation (X, Y, and LOD) are shown in Figure 2 after removing the contributions from winds [Salstein and Rosen, 1997] and ocean currents [Johnson et al., 1999], along with the results from LAGEOS SLR observation. Best estimates of the geophysical contributions from atmospheric surface pressure, continental water storage, and non-steric sea level change are also shown [Chen at al., 2000a]. The interannual variations of the three independent estimates (Earth rotation, LAGEOS SLR, and geophysical models) are shown in Figure 3. Figure 4 shows cross correlations among the three estimates for interannual C21, S21, and C20 variations.

The three estimates have reasonable agreement at a broad band of frequencies, especially among the seasonal variations of S21 and C20. The C21 variations show poorer agreement, which is likely due to the weaker seasonal variability of C21 (~30-50% less than C20 and S21). The weaker C21 variations, corresponding to the mass-induced excitations of polar motion X, are generally attributed to the geographic distribution of the continents, which are more closely aligned to the Y-axis. Therefore, the S21 variations (or Y excitations) are more sensitive to the seasonal mass variations over the continents, which include atmospheric surface pressure and continental water storage changes. The C21 axis is aligned through the oceans and the pressure variations over the oceans are more or less canceled out by the IB effects, although IB effects are still not completely understood and are still under investigation.

The strong seasonal variability in the C20 variation is due to the well-known large-scale zonal patterns in atmospheric, oceanic, and hydrologic general circulation systems. The C_{20}^{SLR} estimate agrees better with the geophysical model predictions in both amplitude and phase compared to the LOD-derived results. The better performance of LAGEOS SLR tracking data in determining the degree 2 zonal term, i.e., C20, is not surprising. This is because the variations are the best determined gravitational change by LAGEOS SLR data owing to the natural sensitivity of LAGEOS to C20 changes via precession of the satellite node. Alsoandwind effects are very dominant in driving LOD variations and must first be removed from the observed LOD variations in order to separate the gravity variations. The latter makes the Earth rotation C20 estimates less accurate than the LAGEOS SLR determinations.

There is a strong peak in Figure 4 (a correlation coefficient estimate of ~0.42) at zero phase lag between $C_{21}^{SPACE\ 97}$ and $C_{21}^{Geophy.}$, while there is no notable peak between C_{21}^{SLR} and $C_{21}^{Geophy.}$. The peak correlation coefficient between $S_{21}^{SPACE97}$ and $S_{21}^{Geophy.}$ is as large as 0.82 compared with the peak value 0.28 between S_{21}^{SLR} and $S_{21}^{Geophy.}$. However, both $C_{20}^{SPACE97}$ and C_{20}^{SLR} are strongly correlated with $C_{20}^{Geophy.}$. We have also computed the power spectral density of the three estimates of C21, S21, and C20 in order to better examine the variability (Figure 5). The power spectra indicate that the $C_{21}^{SPACE\ 97}$ and $S_{21}^{SPACE97}$ estimates are more similar with geophysical model predictions in most of the frequencies examined (from annual or 1 cycle/yr to 15 cycles/yr), than with the SLR estimates. The C_{21}^{SLR} and $S_{21}^{Geophy.}$ estimates show higher annual amplitudes (Figure 3) than the other estimates. The results suggest that polar motion X and Y have the potential

to be more accurate than LAGEOS SLR tracking in determining C21 and S21 variations, especially at interannual timescales. However, the LAGEOS SLR tracking has been demonstrated to be more reliable than the LOD measurements in deriving the C20 variations.

Work is ongoing to assess the reasons for these differences by examining different ocean models to correct the Earth rotation parameters for the motion terms and different hydrological models for the geophysical estimates. Also, the results from new multi-satellite solutions [Cheng and Tapley, 1999] are being examined to see if there are improvements in the C21 and S21 terms.

2.2.2 Variability and Excitation of Polar Motion

We have continued to examine polar motion time series at frequencies beyond the seasonal cycle. Three distinct regimes have been examined: (1) The quasi-biennial, which arises separately from tropospheric and stratospheric origins, (2) the triennial-quadrennial, is also related to the El Niño/Southern Oscillation signals, and (3) a six-year period [Abarca del Rio et al., 2000]. There are slight difference in time scales of the quasi-biennial oscillations which are more apparent during years with strong El Niño events. We have examined the regional and vertical propagation of the so-called triennial-quadrennial signals within the atmosphere. Our studies also indicate that the six-year period is not related to the atmosphere; we theorize that it may be driven by core-mantle interactions of the Earth.

Variations on much shorter time-scales have also been examined. We have found that polar motion is excited by atmospheric mass fluctuations down to the order of about one week [Salstein, 1999] (Figure 6). The wind excitation terms also have an important diurnal signature that must be considered at that time scale. Dynamic forecasts of polar motion excitation have shown positive skill out to 10 days. An article is being submitted to EOS, Transactions of the American Geophysical Union in which we discuss the importance of taking into account accurate representations of high frequency (several days to diurnal) variability to adequately model the high frequency motions of the Earth, related to nutation [Salstein et al., 2000].

A study has been conducted relating regional patterns in the atmosphere and ocean to polar motion forcing [Nastula et al., 1999]. Results confirm findings that oceans supplement the atmosphere as an important source for polar motion excitation, with regional signals in the oceanic bottom pressure forcing of somewhat similar magnitude as those in atmospheric forcing. Another study [de Viron et al., 2000] has examined the calculation of ocean torques relevant for nutation using a dynamic barotropic ocean model forced by surface atmospheric winds and pressure. An eigenvector analysis has been applied the polar motion excitation terms to discover regions which explain the most variance [Nastula and Salstein, 1999]. For example, regions related to the mass term of the atmosphere are important over the North Pacific and the Southern Oceans on subseasonal time scales. When the inverted barometer relationship is considered, which is the more likely scenario for polar motion excitation on these scales, the areas over the continents, particularly Eurasia, become more important.

22.3 Angular Momentum Variations

The relationship between Oceanic Angular Momentum (OAM) and Atmospheric Angular Momentum (AAM) to Earth Angular Momentum (EAM) continue to be studied. Values calculated from an ocean data assimilation procedure have been examined [Ponte et al., 2000]. (Figure 7) The assimilation model yields substantial changes in ocean angular momentum (OAM) quantities, related to adjustments in both motion and mass fields, as well as in the wind stress torques acting on the ocean. Constrained OAM values provide noticeable improvements in the agreement with the observed Earth rotation parameters, particularly at the seasonal time scale.

40 years of NCEP/NCAR reanalysis products have been used to calculate separate land and ocean torques, so that their relative importance in driving atmospheric angular momentum signals can be examined. The atmosphere-ocean-solid Earth momentum exchange based on the separated ocean and land torques is also being examined [Ponte and Rosen, in preparation, 2000]. Land torques are found to be the dominant driving mechanism for AAM at intraseasonal and shorter time scales, but ocean torques are as important as land torques at periods of 3 months and longer. Ocean interactions cannot explain, however, the observed phase lead of AAM over LOD at seasonal to intraseasonal timescales.

We have also compared results from several models in order to quantify error in the AM measurements. In one study [Kosek et al., 2000], equatorial excitation functions computed by different meteorological centers were intercompared. Comparing the mean spread within the ensemble from seven meteorological centers to the mean temporal variation yields a larger signal for the pressure than for the wind excitation terms that force polar motion. In a related study [Salstein and Rosen, 1999], we attempted to include as much of the atmosphere as possible, as high as most stratospheric levels. Here we examined the coherence between the major reanalysis-based angular momentum series, to note a decrease of coherence on the highest frequencies between the series from these centers. However, correlation between the tendencies of AAM, i.e., the difference between a parameter's value and its value a certain time lag before, is statistically significant at lag times as short as 0.5 days (Figure 8). The stratosphere is important particularly at the semiannual and quasi-biennial time scales. Also, the planetary axial angular momentum budget on seasonal time scales is reasonably well closed. However, the difference between the seasonal angular momentum of the atmosphere and that in the solid Earth, as noted by LOD measurements, has a power on the same order of magnitude as that of ocean excitations, on these time scales.

We have also examined atmospheric angular momentum based on model simulations submitted to the Atmospheric Model Intercomparison Project (AMIP) [Salstein et al., 1999]. AMIP is a multiyear simulation driven by a given observed sea surface temperature alone. In this task, we are examining the models that are contributing to the second phase (covering 17 years) of this project. Comparisons between the AMIP-2 results and those from the earlier 10-year AMIP-1 experiment indicate an improvement in the newer models. However, the current study is based on

only two models. Moreover, these two models have been supplemented already by a number of other model simulations. We await the opportunity to perform a comprehensive study of model availability with the approximately 30 models that are due to become available within a year.

2.3 Seasonal Continental Water Storage

Quantification of continental water storage change has significant contributions to the study of the Earth system dynamical changes. We have assessed continental water storage changes at seasonal scales using output from using four different hydrological models. The amplitude and phase of seasonal continental water storage change at each grid point is computed, and the results from the four models are compared at different spatial scales.

The four hydrological models to be analyzed include soil moisture and snow data from the NCEP-NCAR Data Assimilation System 1 (CDAS-1), ECMWF operational forecast system, and a climatological archive compiled by Willmott and Rowe [1985], and precipitation and evaporation data from NASA GEOS-1 assimilation system. Global surface runoff data is from a seasonal average compiled by Oki et al. [1997]. Details about the four hydrological models and data processing can be found in Chen et al. [2000b]. Figure 9 shows the annual amplitudes of continental water storage change for the 4 different hydrological models. The annual phases (with respect to January 1) from the four models are shown in Figure 10. Antarctica and Greenland are excluded in this comparison.

Discrepancies between the four models are quite obvious. CDAS-1 and GEOS-1 over-estimate seasonal continental water storage change, especially CDAS-1. The annual amplitude from CDAS-1 soil and snow water is nearly 2-3 times larger than other models. The ECMWF model derived seasonal variability is in good agreement with Willmott's climatology. There is reasonable agreement in phase between the four models. This study shows that seasonal discrepancies at several cm level exist in many regions with spatial scale of several hundred to a few thousand kilometers, indicating the immaturity of current hydrological models and the need of intensive study in understanding and modeling water mass variation within the Earth system. Plans are to continue the examination of the hydrological models on interannual time scales.

2.4 Ocean Steric Model and Ocean Mass Variations

Work has continued on estimating ocean mass variations from satellite altimetry after removing a steric model. Previously, we have used a steric model based on climatology [Chen et al., 2000c] which is only useful for studying the seasonal signals [Chen et al., 1998]. The Chen et al. [1998] study did show qualitative agreement between hydrological and atmospheric models and the altimeter measurements on global space-scales and seasonal periods.

7

Over the last year, we have been studying the use of direct measurements of the steric variability made by eXpendable BathyThermagraphs (XBTs) during the TOPEX/Poseidon (T/P) time frame [Chambers et al., 1999; Chambers et al., 2000]. The XBT data are sparse, but we have been able to interpolate the data to uniform, global maps using a method known as empirical orthogonal function (EOF) reconstruction (Figure 11). The global, seasonal signal of sea level change due to ocean mass variations determined with this new model agrees well with our previous study (Figure 12). In addition, because the new XBT-derived steric model contains interannual signals, we have also been able to study interannual ocean mass changes (Figure 13). An analysis has been performed on the interannual variability [Chambers et al., 2000] and the results indicate that the ocean lost an equivalent of 18 mm of MSL between 1995 and 1997 due to fresh water loss. This result is significant at the 95% confidence level based on an error analysis. The steric expansion was even larger, though, so global mean sea level still rose by nearly 20 mm during the 1997 El Niño [Nerem et al., 1999] (Figure 14). The timing of the initiation of the water loss cycle preceded the 1997 El Niño by nearly a year. Its connection with the dynamics of El Niño, if any, is unknown but is under investigation.

A comparison of the measured interannual oceanic water mass variations and the output from numerical models shows very little agreement (Figure 15), unlike with the seasonal signal [Chen et al., 1998]. Although the magnitude of change predicted by the model can be as large as what is observed, the phasing is very different. These results suggest that the current models are inadequate for resolving interannual variations in the hydrological cycle.

Although we have found that the global ocean water mass variations can be determined from altimetry with some degree of accuracy, we have just started to examine smaller-scales, such as basin-scales or less. Errors will increase, mainly because of local, unmeasured salinity and barotropic effects which generally average out on global-scales, so the corresponding water mass variation must also be larger in order to be measurable with this technique. Examination of the barotropic signal from an ocean model [Ponte, 1999] indicates significant barotropic signals in only a few locations (Figure 16). However, local salinity effects can be relatively large, and are generally unmeasured.

The GRACE mission is expected to be able to detect geoid changes associated with water mass changes at the few mm level [Wahr et al., 1998]. In the next several years, we will be able to verify the altimeter-steric measurement against the GRACE measurements. In the meantime, we are beginning to examine the time-varying geoid determined from the 5x5 15-day gravity field solutions determined from SLR and DORIS data [Cheng et al., 2000], and use this as a check against the altimeter-steric measurements. We hope to be able to quantify both seasonal and interannual geoid changes on at least basin-scales before the launch of GRACE in 2001.

2.5 Mass Signals Observable by GRACE

High-altitude satellites such as LAGEOS have demonstrated that the time-varying gravity field at long spatial wavelengths can be attributed to mass redistribution within

the Earth's system, especially in the atmosphere, hydrosphere, and oceans [Chen et al, 1999, Cazenave et al., 1999; Nerem, et al., 2000]. Little has been observed of the time-varying gravity field at shorter wavelengths. The GRACE mission was designed to measure the gravity variations at wavelengths down to a few hundred km, and it is expected that the measurements from GRACE will provide significant improvements in our ability to measure the exchange of mass between the Earth system components. In preparation for the GRACE mission, we have considered the types of mass signals one can expect to see from GRACE.

General circulation models offer a way to assess the impact of mass changes on the gravity field due to the redistribution of various Earth system components [Wahr et al., 1998]. In this way, the prospects for detecting climate signals in the gravity field by satellite gravity missions, such as GRACE, can be assessed. Using monthly-averaged fluid mass diagnostics from a coupled atmosphere-ocean model (AOM) developed at the Goddard Institute for Space Studies (GISS) [Russell et al. 1995], geoid variations have been estimated from the fundamental model mass components. From these estimates, the seasonal geoid signals from sea level, snow, sea ice, soil moisture, water vapor, and surface pressure can be compared to estimated errors for GRACE. In addition, the impact of increasing greenhouse gases can be assessed by comparing model results both with and without increasing CO_2 and with varying tropospheric sulfate aerosols [Leuliette et al. 2000]. An important feature of this model is that it is mass conserving; i.e., water mass is neither lost nor gained, but is moved among the Earth system components.

Three simulations of the AOM have been analyzed: a control simulation with a constant 1950 atmospheric composition (C089), a simulation using observed greenhouse gases for 1950–1990 and 0.5% CO_2 annual increases thereafter (C090), and a simulation with the greenhouse gases of C090 with UKMO tropospheric sulfate aerosol changes (C091). The AOM's seasonal changes for 1965–1995 compare favorably with observed surface temperature changes. The simulation C091 results in a cooler climate than C090 because sulfate aerosols increase significantly until year 2050 with a slight decrease thereafter. The seasonal regional temperature changes for the past 40 years show strong positive spatial correlation between C090 minus C089 and the observations in the northern hemisphere. C091 minus C089 shows weaker correlations [Russell et al., 2000].

The annually-varying gravity signals predicted by the GISS AOM for ocean and sea ice, surface pressure, soil moisture, and snow mass changes are well above the preliminary GRACE measurement errors at half wavelengths ranging from 1000 to 10000 km (Figure 17). Therefore, GRACE measurements will likely provide a useful boundary condition for annual mass variations in coupled climate models.

The GISS AOM's strengths are its ability to simulate seasonal and secular changes in climate. However, interannual variations of continental water storage have large fluctuations at many spatial scales, similar to the problem of estimating secular sea level change using satellite altimetry [Nerem et al., 1999]. Large, unmodeled interannual changes would increase the uncertainty in recovering the secular change in the geoid over the five-year duration of the GRACE mission. To assess the impact of these interannual fluctuations on the recovery of secular trends in the geoid, we have used a terrestrial

water storage dataset generated from a Geophysical Fluid Dynamics Laboratory (GFDL) general circulation model [Milly and Dunne, 1994] to calculate the root-mean-square amplitude of the interannual variations.

The combined error in secular trend recovery from instrument uncertainty, PGR error, and interannual variations is shown in Figure 18. The effect of these errors is dependent both on the length of the available time series and the extent of the spatial averaging. We have simulated the uncertainties in the secular trend recovery for two cases: a single GRACE mission (five years) and GRACE followed by a comparable mission (ten years).

Mass flows with significant secular trends as calculated from differences in the model runs have been used to estimate the magnitude of climate change over five years. These mass redistributions should be detectable by GRACE in principle, although these components cannot be separated using GRACE data alone. However, variations in the spatial characteristics of each of the components may allow for their discrimination. Knowledge of the secular variations in gravity could be used for constraining future coupled atmosphere-ocean climate models. In addition, the effect of the aliasing of diurnal mass variations in the ocean and atmosphere from monthly sampling on the determination of interannual periods is a concern and is being studied.

3. PLANNED ACTIVITIES FOR 2000-2001

For completion to this study, we will finish several studies of the Earth's water mass variability under the new grant NAG5-9989. In particular, the variability in each of the Earth systems (ocean, land, and atmosphere) will be assessed and we will continue our efforts to map these changes into changes in the Earth's rotation and angular momentum. In addition, we will examine the size of expected carbon mass variability related to water mass variations, using model output and results from the TERRA instruments. We want to identify areas where carbon mass variability may be the same order, or even larger than water mass variability. In addition, we will continue the investigation into determining ocean heating signals in order to better separate the thermal and mass effects from sea level change, with a focus on smaller scales than global.

4. REFERENCES

Abarca del Rio, R. A., D. Gambis, and D. Salstein, Interannual signals in length of day and atmospheric angular momentum, *Ann. Geophysicae, 18,* 347-364, 2000.

Cazenave, A., F. Mercier, F. Bouille, and J. M. Lemoine, Global-scale interactions between solid Earth and its fluid envelopes at the seasonal time scale, *Earth Planet. Sci. Lett.,* 171, 549–559, 1999.

Chambers, D. P., J. L. Chen, and B. D. Tapley Separation of Thermal and Mass Signals in Sea Level Variability by Combining Satellite Altimetry and Expendable

Bathythermagraph Data, presented at 1999 meeting of International Union of Geodesy and Geophysics, Birmingham, U.K., July, 1999.

Chambers, D. P., J. L. Chen, R. S. Nerem, and B. D. Tapley, Global Mean Sea Level Change and the Earth's Water Mass Budget, submitted to *Geophys. Res. Ltrs.*, 2000.

Chen, J. L., Geodynamical Interconnections Between the Atmosphere, Ocean, Hydrosphere, Cryosphere, and Solid Earth, Ph.D. Dissertation, The University of Texas at Austin, December, 1998.

Chen, J. L., C. R. Wilson, D. P. Chambers, R. S. Nerem, and B. D. Tapley, Seasonal global water mass balance and mean sea level variations, *Geophys. Res. Ltrs.*, 25, 3555-3558, 1998.

Chen, J. L., C. R. Wilson, R. J. Eanes, and B. D. Tapley, Geophysical contributions to satellite nodal residual variation, *J. Geophys. Res.*, 104, 23237–23244, 1999.

Chen, J.L., C.R. Wilson, R.J. Eanes, and B.D. Tapley, A New Assessment of Long Wavelength Gravitational Variations, *J. Geophy. Res.*, 2000a (in press).

Chen, J.L., C.R. Wilson, B. D. Tapley, D.P. Chambers, and T. Pekker, Hydrological Impacts on Seasonal Sea Level Change, *Global and Planetary Change*, 2000b (in review).

Chen, J. L., C. K. Shum, C. R. Wilson, D. P. Chambers, and B. D. Tapley, Seasonal sea level change from TOPEX/Poseidon observation and thermal contribution, *J. Geodesy*, 73, 638-647, 2000c.

Cheng, M. K. and B. D. Tapley, Seasonal variations in low degree zonal harmonics of the Earth's gravity field from satellite laser ranging observations, *J. Geophys Res.*, 104(B2), 2667-2681, 1999.

deViron, O., C. Bizouard, D. Salstein, and V. Dehant, Atmospheric torque on the Earth and comparison with atmospheric angular momentum variation, *J. Geophys. Res.* 104, 4861-4875.

de Viron, O., R.M. Ponte, and V. Dehant, Indirect effect of the atmosphere on the Earth nutation by the torque approach, submitted to *J. Geophys. Res.*, 2000.

Douglas, B. C., Global sea level rise, *J. Geophys. Res.*, 96, 6981-6992, 1991.

Gross, R. S., Combinations of Earth orientation measurements: SPACE94, COMB94, and POLE94, *J. Geophys. Res.*, Vol.101, B4, 8729 - 8740, 1996.

Hansen, J., R. Ruedy, M. Sato, and R. Reynolds, Global surface air temperature in 1995: Return to pre-Pinatubo level, *Geophys. Res. Lett.*, 23, 1665–1668, 1996.

Iskenderian, H. and D. Salstein, Regional sources of mountain torque variability and high-frequency fluctuations in atmospheric angular momentum, *Mon. Wea. Rev.*, 1681-1694, 1998.

Kosek, W., D. Salstein, and W. Popinski, Comparison of the equatorial EAAM excitation functions computed by different meteorological centers using time variable coherence/correlation approaches, presented at European Geophysical Society XXV General Assembly, Nice, France, 2000.

Leuliette, E. W., R. S. Nerem, and G. L. Russell, Detecting time variations in gravity associated with climate change, submitted to *J. Geophys. Res.*, 2000.

Mehlhaff, C. A., D. P. Chambers, and R. S. Nerem, Reconstruction of historical global mean sea level change using empirical orthogonal functions, presented at 2000 Ocean Sciences Meeting, January, 2000.

Milly, P. C. D., and K. A. Dunne, Sensitivity of the global water cycle to the water-holding capacity of land, *J. Climate*, 7, 506–526, 1994.

11

Nastula, J., and D. Salstein, Regional atmospheric patterns in polar motion excitation, presented at Fall AGU meeting, 1998.

Nastula, J. and Salstein, D., Regional atmospheric angular momentum contributions to polar motion excitation, *J. Geophys. Res., 104*, 7374-7358, 1999.

Nastula, J. and D. Salstein, Modes of variability in high-frequency atmospheric excitation for polar motion, presented at European Geophysical Society XXV General Assembly, Nice, France, 2000.

Nastula, J., R.M. Ponte, and D. Salstein, Regional signals in atmospheric and oceanic excitation of polar motion, presented at International Astronomical Union Symposium No. 178: Polar Motion, Historical and Scientific Problems, 1999.

Nerem, R. S., D. P. Chambers, E. W. Leuliette, G. T. Mitchum, and B. S. Giese, Variations in global mean sea level associated with the 1997-98 ENSO event, submitted to *Geophys. Res. Lett.,* 1999.

Nerem, R. S., R. J. Eanes, P. Thompson, and J. L. Chen, Observations of annual variations of the Earth's gravitational field using satellite laser ranging and geophysical models, submitted to *Geophys. Res. Lett.,* 2000.

Oki, T., T. Nishimura and P. Dirmeyer, Validating Estimates of Land Surface Parameterizations by Annual Discharge using Total Runoff Integrating Pathways, *J. of Japan Soc. of Hydrol. and Water Resour.,* 9, 416-425, 1997.

Ponte, R. M., A preliminary model study of the large-scale seasonal cycle in bottom pressure over the global ocean, *J. Geophys. Res.,* 104 (C1), 1289-1300, 1999.

Ponte, R.M., and D. Stammer, Importance of oceanic excitation of polar motion at seasonal and shorter periods, AGU Fall Meeting, San Francisco, 1998.

Ponte, R.M., and D. Stammer, Role of ocean currents and bottom pressure variability on seasonal polar motion, *J. Geophys. Res.,* submitted, 1999a.

Ponte, R.M., and D. Stammer, Regional signals in ocean currents and bottom pressure, in relation to the Earth's angular momentum, AGU Spring Meeting, Boston, 1999b.

Ponte, R. M., D. Stammer, and J. Marshall, Oceanic signals in observed motions of the Earth's pole of rotation, *Nature, 391*, 476--479, 1998.

Ponte, R., D. Stammer, and C. Wunsch, Estimating ocean angular momentum using a general circulation model constrained by data, presented at European Geophysical Society XXV General Assembly, Nice, France, 2000.

Russell, G. L., J. R. Miller, and D. Rind, A coupled atmosphere-ocean model for transient climate change, *Atmo.-Ocean, 33*, 683–730, 1995.

Russell, G. L., J. R. Miller, D. Rind, R. A. Ruedy, G. A. Schmidt, and S. Sheth, Comparison of model and observed regional temperature changes during the past 40 years , *J. Geophys. Res.,* in press, 2000.

Salstein, D. A., Atmospheric excitation of polar motion, presented at International Astronomical Union Symposium No. 178: Polar Motion, Historical and Scientific Problems, 1999.

Salstein, D. A., and R. D. Rosen, Global momentum and energy signals from reanalysis systems. *7th Conf. on Climate Variations,* American Meteorological Society, Boston, MA, 344-348, 1997.

Salstein, D. A. and R. D. Rosen, Atmospheric angular momentum during the 1997-98 El Niño Event., Proceedings, *23rd annual NOAA Climate Diagnostics and Prediction Workshop,* 58-61, 1998.

Salstein, D. A. and R. D. Rosen, Sources of uncertainty in current atmospheric angular momentum time series, presented at Fall Meeting of American Geophysical Union, San Francisco, CA, 1999.

Salstein, D. A. and A. J. Miller, Special Bureau for the Atmosphere. Submitted to *International Earth Rotation Service Technical Note*, 1999.

Salstein, D., R. Rosen, J. Dickey, and S. Marcus, Assessing atmospheric general circulation models using angular momentum diagnostics, presented at 1999 meeting of International Union of Geodesy and Geophysics, Birmingham, U.K., July, 1999.

Salstein, D., O. de Viron, M. Yseboodt, V. Dehant, Urging an improvement of diurnal atmospheric and oceanic modeling for excitations of high-frequency Earth orientation parameters, in submission to *EOS, Transactions of the American Geophysical Union*, 2000.

Smith T. M., R. W. Reynolds, R. E. Livezey, and D. C. Stokes, Reconstruction of historical sea surface temperatures using empirical orthogonal functions, *J. Climate, 9*, 1403-1420, 1996.

Trenberth, K. E. and C. J. Guillemot, The total mass of the atmosphere, *J. Geophys. Res.*, Vol. 99, D11, 23079 – 23088, 1994.

Urban, T. J., T. Pekker, C. K. Shum, G. L. H. Kruizinga, and B. D. Tapley, A Multi-Year Accuracy Assessment of Wet Troposphere Correction from TOPEX/Poseidon, ERS-1, and ERS-2 Microwave Radiometer, submitted to *J. Geophys. Res.*, 1999.

Van den Dool, H. M., S. Saha, J. Schemn, and J. Huang, A temporal interpolation method to obtain hourly atmospheric surface pressure tides in reanalysis 1979-1995, *J. Geophys. Res.*, 1998.

Wahr, J., M. Molenaar, and F. Bryan, Time-variability of the Earth's gravity field: Hydrological and oceanic effects and their possible detection using GRACE, *J. Geophys. Res., 103*, 32,205–30,229, 1998.

Willmott, C. J., C. M. Rowe, and Y. Mintz, Climatology of the terrestrial seasonal water cycle, *J. Climatology*, 5,589-606, 1985.
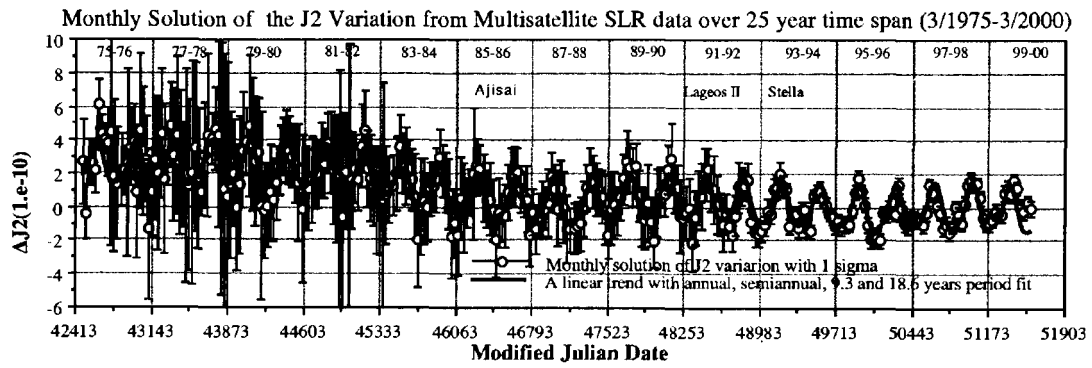
Figure 1. Time series of mass redistribution sensed by J2 from multi-satellite solution.
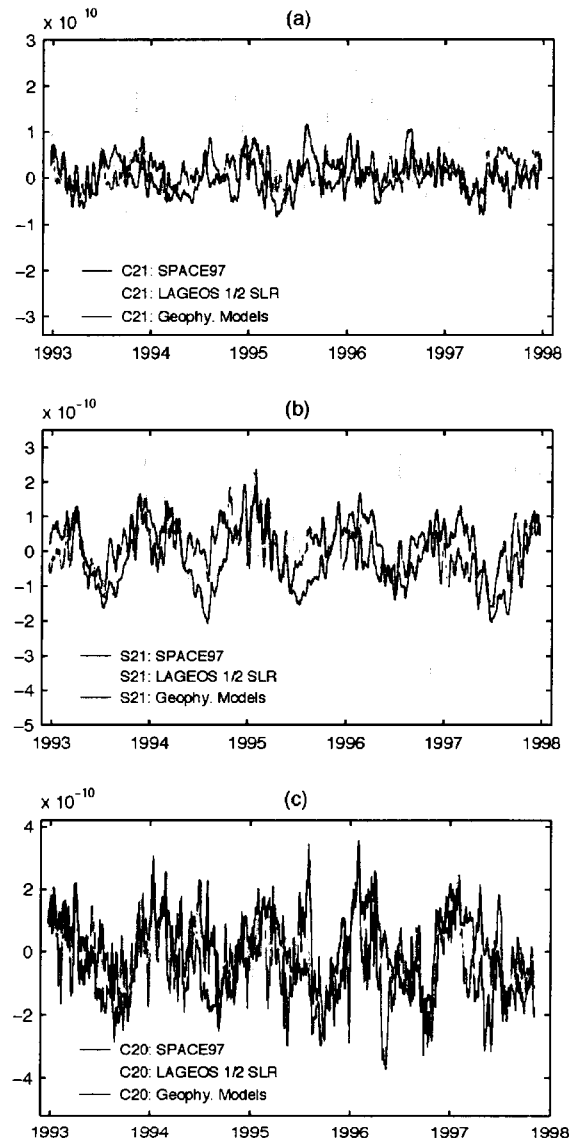
Figure 2. Estimates of the C21, S21, and C20 variations based on SPACE97 X, Y, and LOD, LAGEOS 1/2 SLR data, and geophysical models.
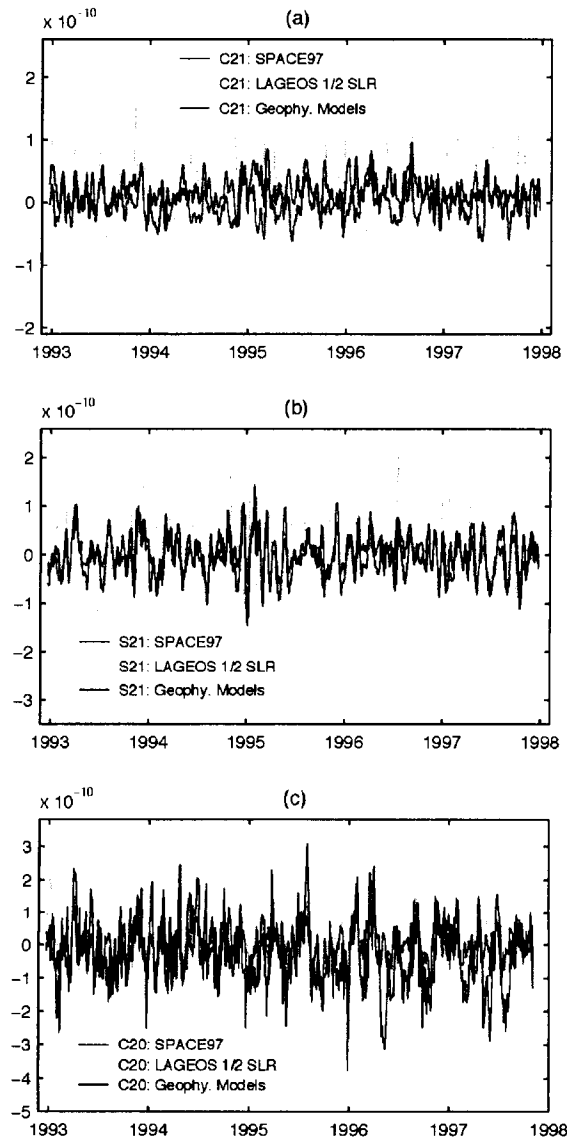
Figure 3. Interannual C21, S21, and C20 variations based on SPACE97 X, Y, and LOD, LAGEOS 1/2 SLR data, and geophysical models.
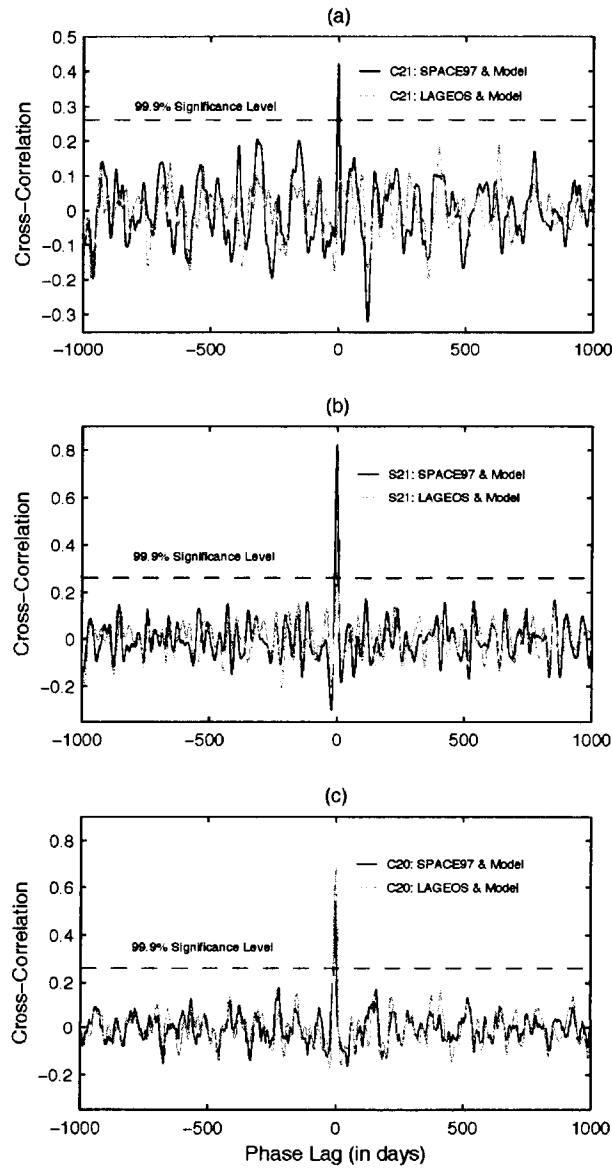
16

Figure 4. Cross correlation analysis for interannual C21, S21, and C20 variations between Space97 estimates and geophysical model predictions (solid curves), and between LAGEOS 1/2 SLR solutions and geophysical model predictions (dashed curves).

17
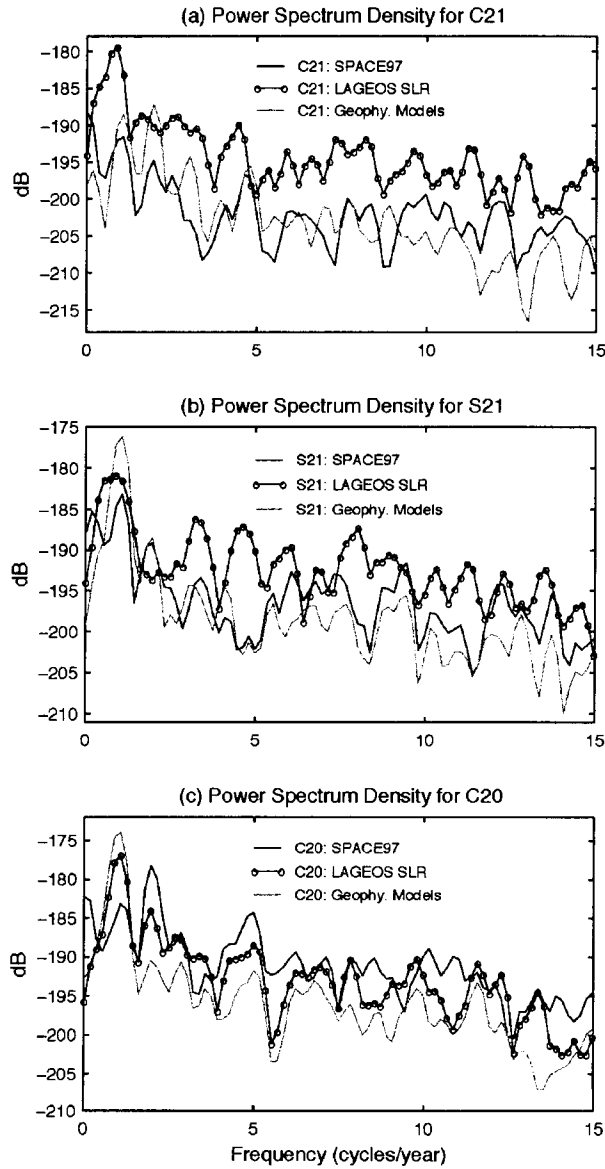
Figure 5. Power spectral density for (a) C21, (b) S21, and (c) C20 variations estimated from SPACE97 (solid curves), LAGEOS 1/2 SLR (solid curves with circles), and geophysical models (dashed curves).

18
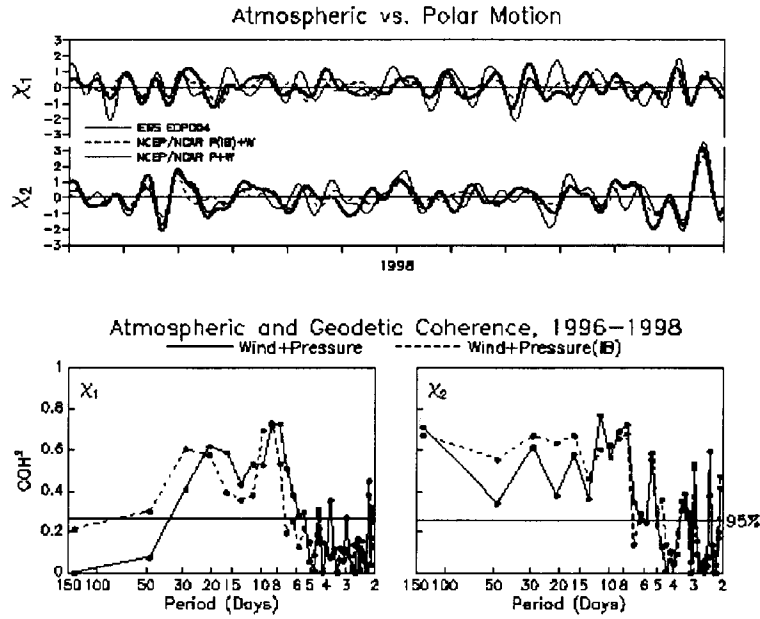
Figure 6 **(Top)** A comparison of geodetic and atmospheric (including or not the IB) and geodetic excitations for polar motion, filtered between 14 and 40 days for the year 1998. Units are non-dimensional times 10^{-7}. **(Bottom)** Coherence between geodetic and atmospheric terms (including or not the IB) between 2 and 150 days. The horizontal line gives the measure of 95% significance.
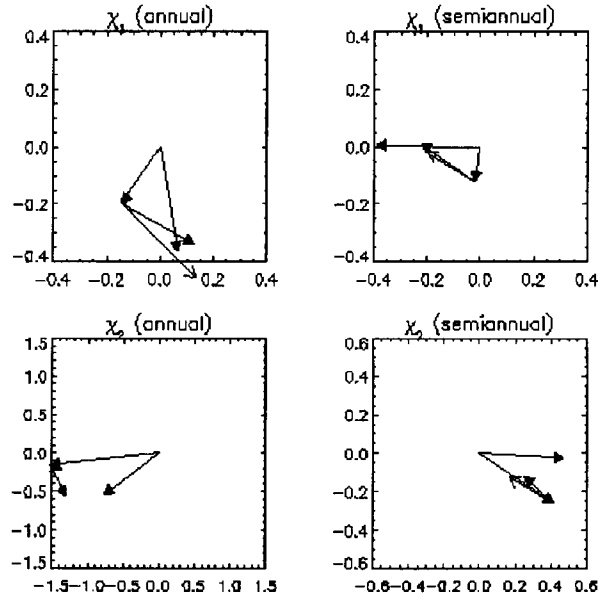
Figure 7. Phasor diagram for annual and semiannual wobble excitation in the two equatorial components of polar motion excitation. Vectors represent dimensionless amplitudes times and phases of geodetic (observed), atmospheric, and oceanic excitation. An arrow pointing due east (south) denotes a maximum on January 1 (April 1). The geodetic (observed) and atmospheric vectors share the origin, and the oceanic term is added to the atmospheric. Solid (open) arrows denote the oceanic term with (without) data assimilation.

19

Coherence and Tendency Correlation
Between NCEP/NCAR and ERA $M^W(10)$
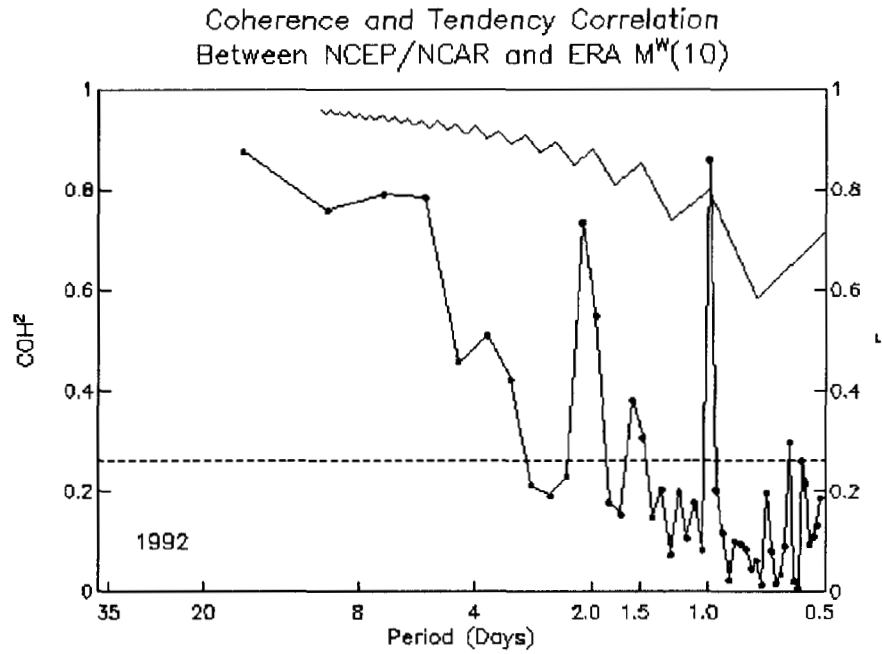
Figure 8. Black line indicates the coherence between angular momentum series from two atmosphere analyses (the NCEP/NCAR and European Center Reanalyses). The red curve indicates the correlation between the tendencies of these same two series. Tendency at lag tn is defined as the value at time t + tn minus the value at time t.

20
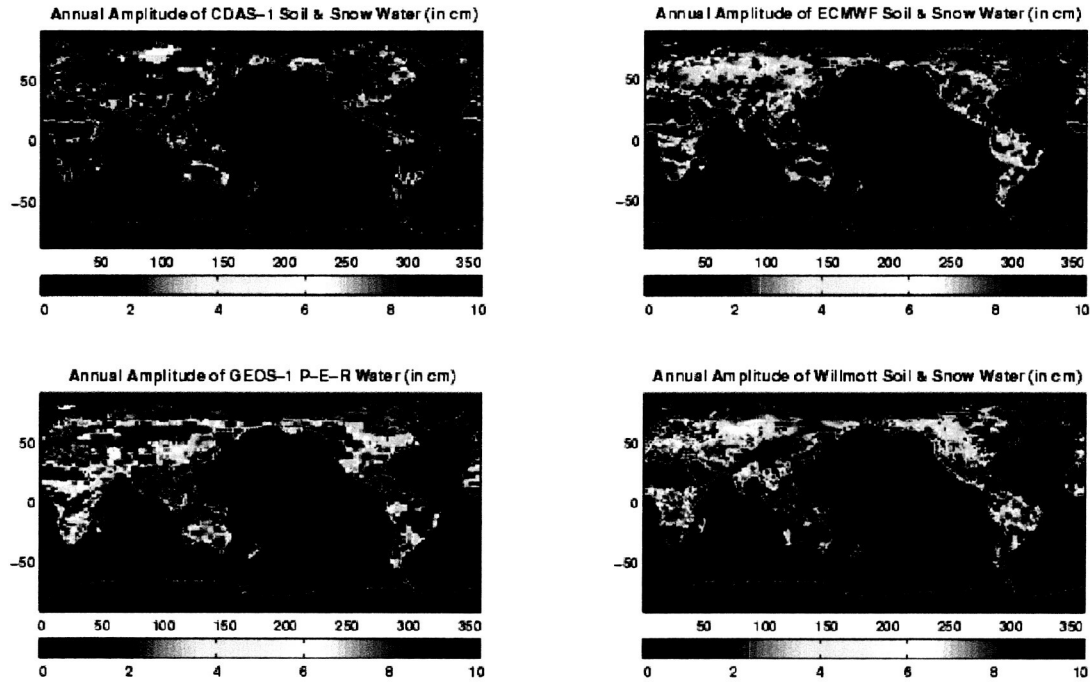
Figure 9. Annual amplitude (in cm of water) estimated from four different hydrological models [Chen et al., 2000b].
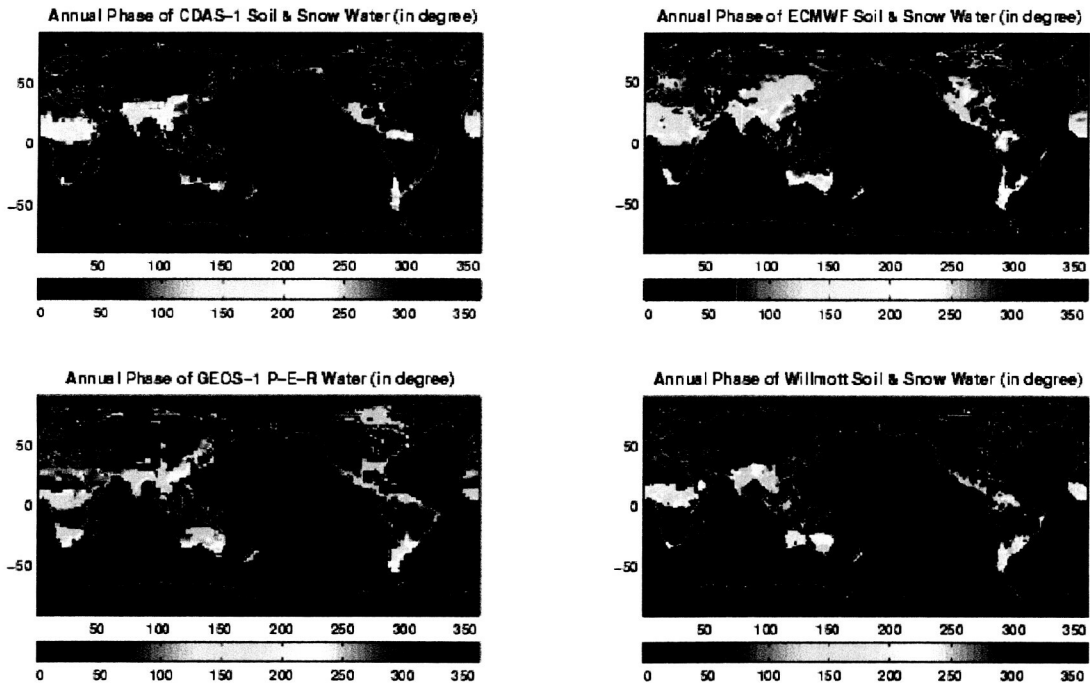
Figure 10. Annual phase (days with respect to January 1) estimated from four different hydrological models [Chen et al., 2000b].
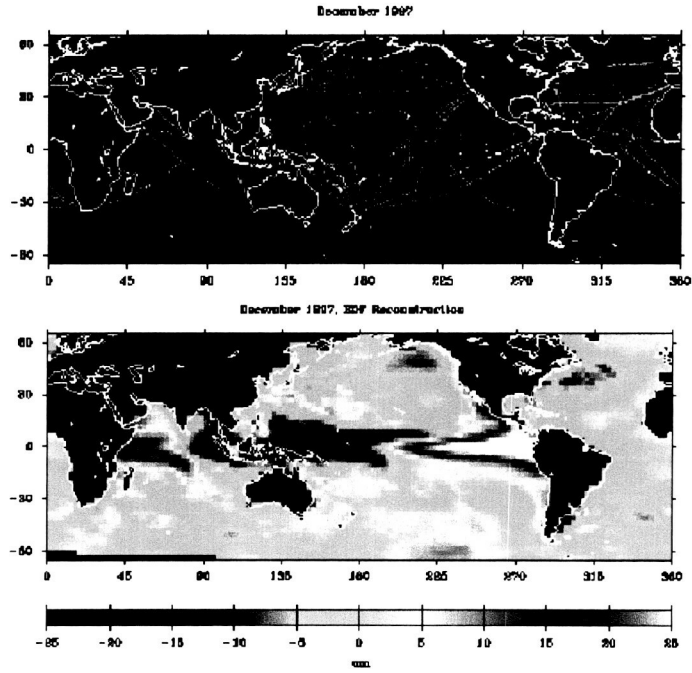
Figure 11. 2.5° gridded XBT sea level anomalies (top) and grid interpolated with EOF Reconstruction (bottom).
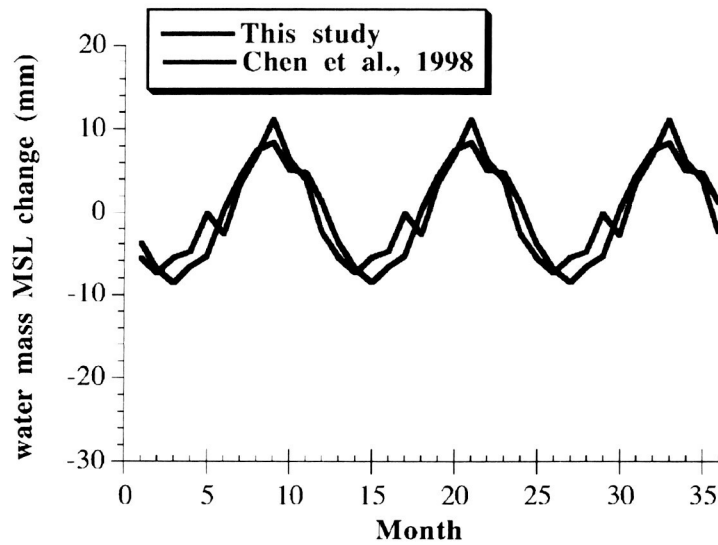
Figure 12. Seasonal global mean sea level variation due to fresh water flux using the Chen et al. [1998] climatology model (blue curve) and the Chambers et al. [2000] XBT model (red curve).
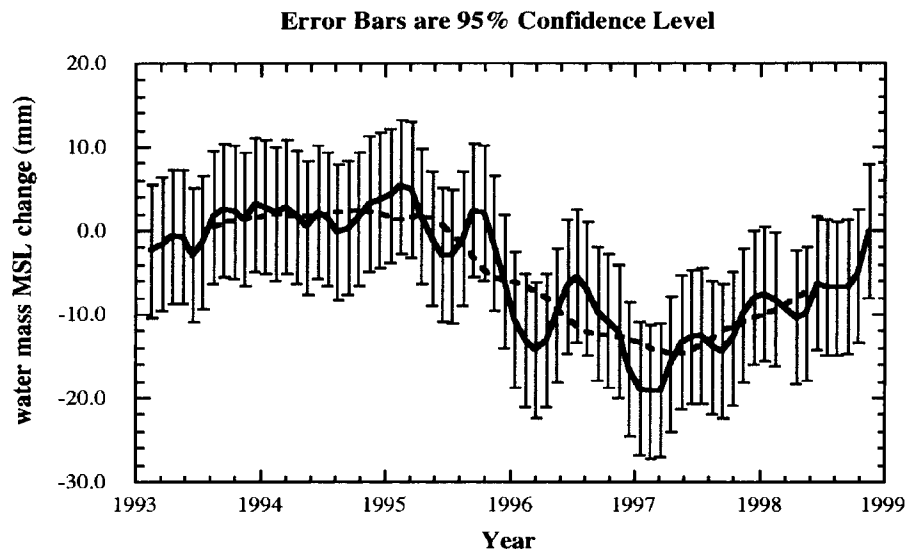
Figure 13. Interannual global mean sea level variation due to fresh water flux using the Chambers et al. [2000] XBT model. The dashed line is a 1-year running mean.
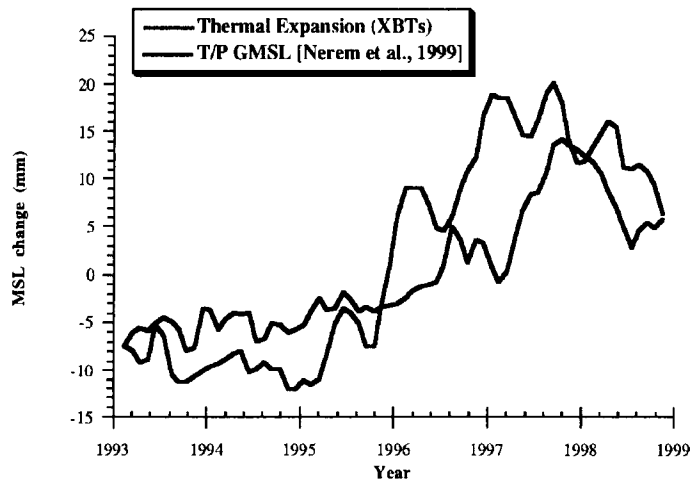

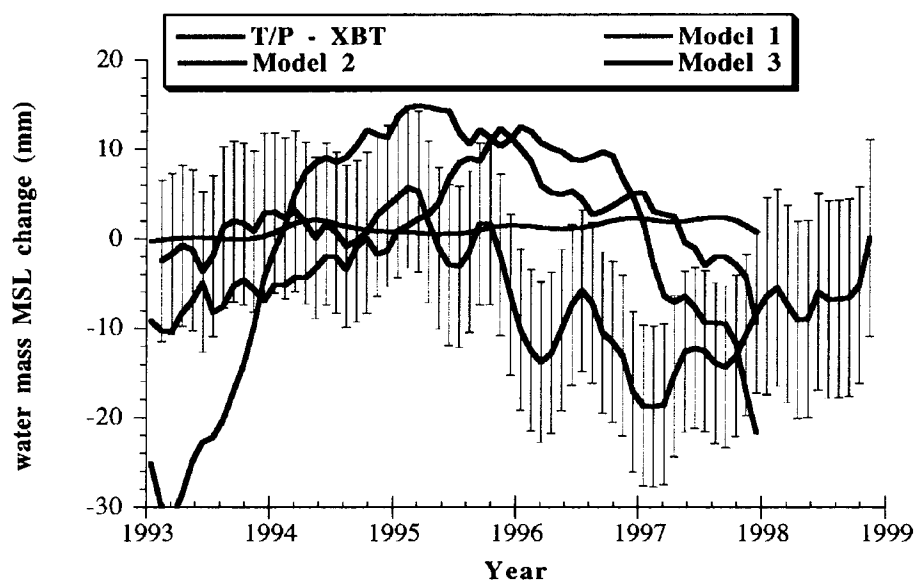**Figure 14**. GMSL due to thermal expansion as measured by XBTs and total GMSL measured by T/P.

Figure 15. GMSL due to fresh water flux as measured by T/P with a steric correction (red curve) and as computed from three numerical models.
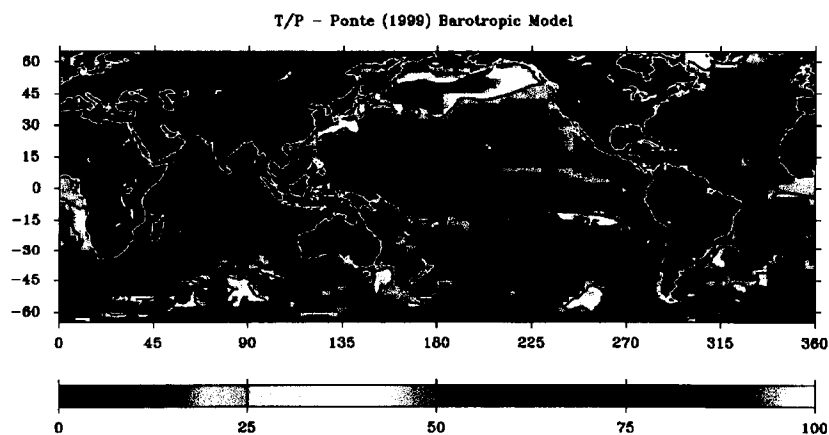

Figure 16. Percent of total sea level variance explained by barotropic variability (from a model run by Ponte [1999]).
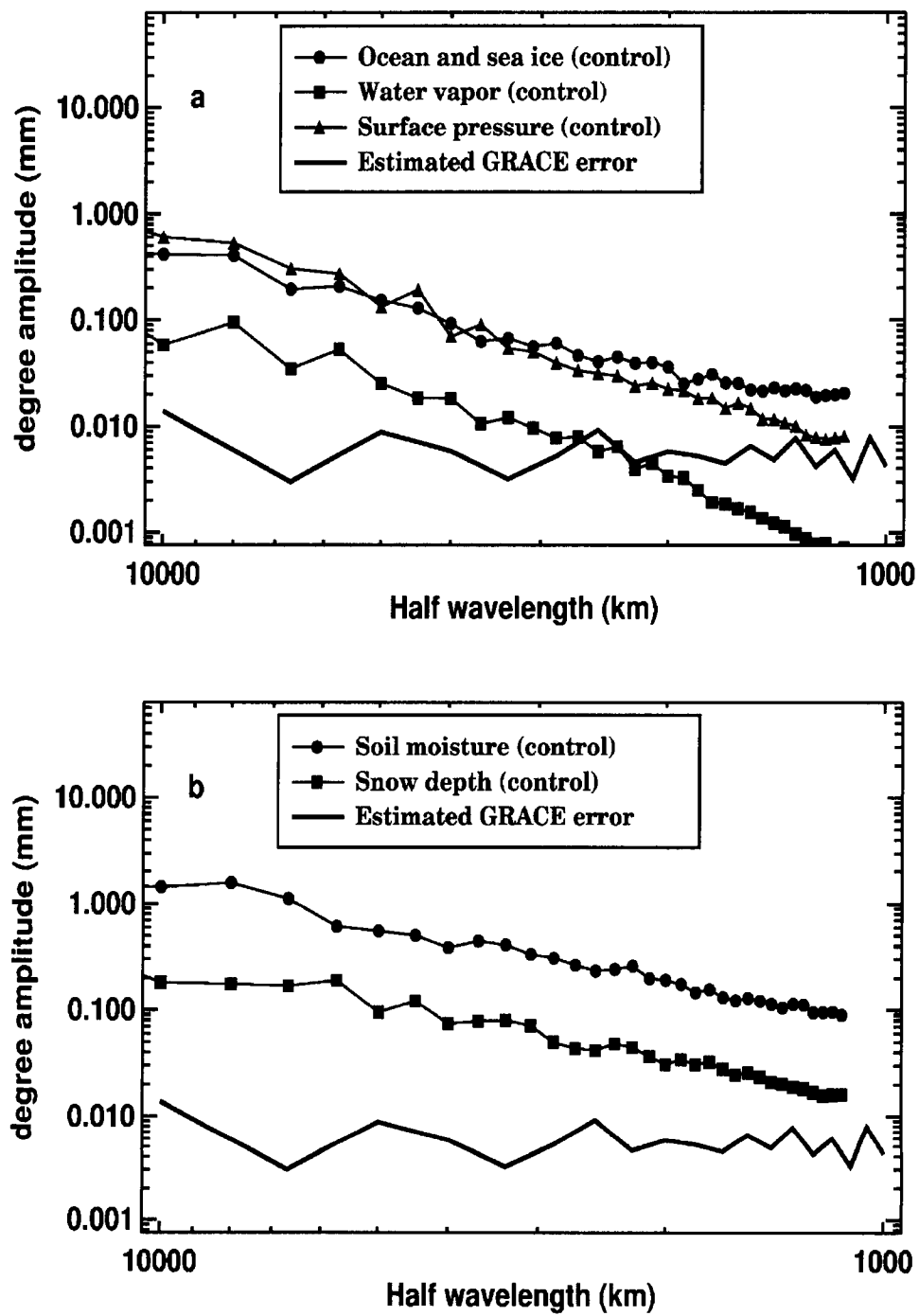
24

Figure 17. Degree amplitudes of the annually-varying geoid as deduced from the GISS AOM control run for a) ocean and atmosphere and b) surface mass changes.
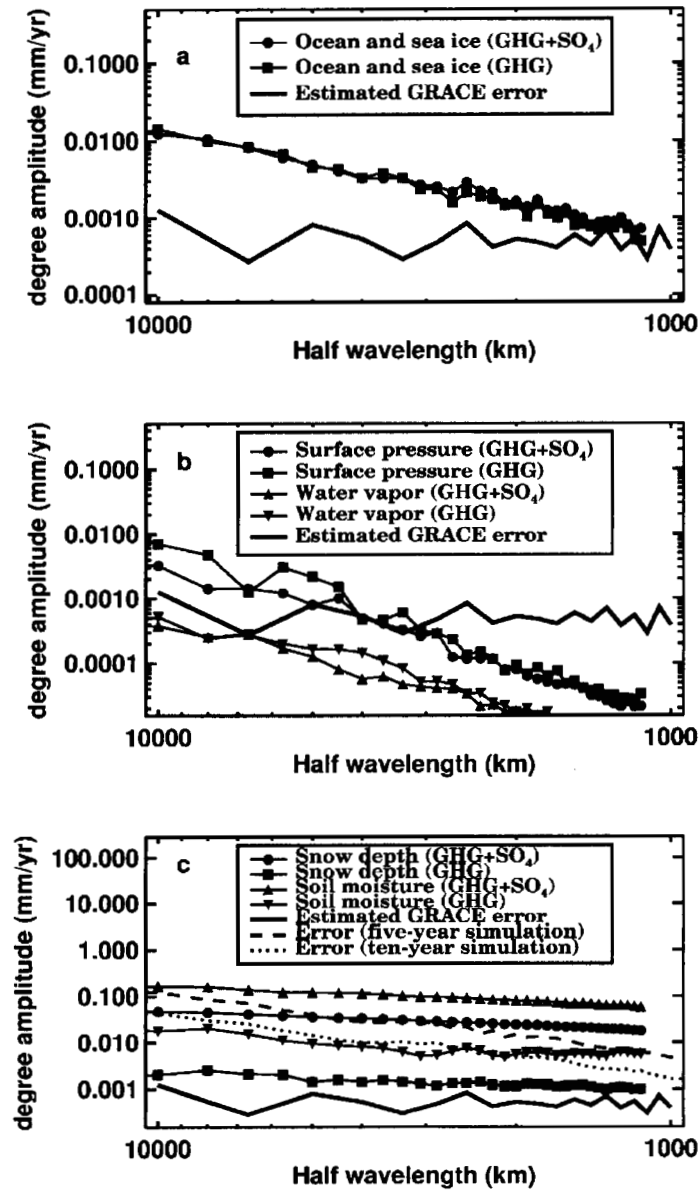
Figure 18. Degree amplitude trends in the geoid as deduced from the GISS AOM climate runs for a) ocean, b) atmosphere, and c) surface mass changes.